

# Geometric Redshift and Light Propagation in a Rotating Lattice Universe

Michael John Sarnowski

June 2025

## Abstract

We propose a cosmological framework in which redshift, lensing, and time dilation emerge from photon propagation through a discrete, rotating lattice composed of spinning Holospheres. Departing from CDM’s reliance on metric expansion and dark energy, this model attributes redshift to a hybrid mechanism: a transverse Doppler-like shift from rotational motion at emission, and exponential phase drag resulting from cumulative angular strain across the lattice.”

Each photon is emitted from a medium moving at a fraction of the speed of light, characterized by its lookback time relative to the total lattice age. As the photon travels toward the outer boundary—into the Holosphere moving at  $c$ —its frequency is modified by the velocity mismatch and rotational tension gradient. The resulting redshift equation provides a physical alternative to metric expansion and naturally reproduces observed acceleration without a cosmological constant. We compare this model against standard cosmological observables, including luminosity distance, angular size, and time dilation, and identify falsifiable predictions that diverge from  $\Lambda$ CDM at high redshift.

## Table of Comments: Overview of Key Contributions and Novel Claims

### 1 Introduction

The standard model of cosmology explains redshift, lensing, and cosmic time dilation through the metric expansion of spacetime, governed by solutions to the Friedmann equations. However, this approach introduces theoretical constructs such as inflation, dark energy, and comoving distances—each carrying unresolved foundational assumptions. In contrast, the Holosphere model proposes that the large-scale structure of the universe is not a continuous metric manifold, but a discrete, rotating lattice composed of fundamental spherical units called Holospheres.

Each Holosphere is a spinning, neutron-scale unit arranged in cuboctahedral packing layers, forming a nested, spherically symmetric structure that defines cosmic geometry and dynamics. As light propagates outward through this rotating lattice, it experiences both transverse motion from spiral emission paths and phase misalignment due to cumulative angular strain. These effects together give rise to redshift, lensing, and coherence variation—without invoking an expanding metric or vacuum energy.

In this model, *rotational strain* plays the central role in shaping observational phenomena. Spin tension gradients between nested shells of Holospheres introduce measurable distortions in photon frequency, trajectory, and coherence. Redshift arises as a hybrid of transverse Doppler-like effects and exponential phase drag through strained orbital channels. Gravitational lensing emerges

from angular tension gradients, rather than mass-induced spacetime curvature. And time dilation transitions from kinetic origin at low redshift to coherence breakdown at high redshift.

This paper develops the observational consequences of this framework. In what follows, we:

- Derive a hybrid redshift equation from the geometry of rotating Holosphere layers.
- Model redshift-distance relations, surface brightness, and angular size without invoking dark energy or expansion.
- Reinterpret lensing, coherence loss, and time dilation as strain-based phenomena in a discrete lattice.
- Identify falsifiable predictions—such as saturation of time dilation, lensing asymmetries, and polarization rotation—that distinguish this model from  $\Lambda$ CDM and tired light theories.

In this model, redshift is not a consequence of stretching spacetime, but of transitioning between media with different effective velocities. Each photon is emitted from a medium composed of spinning Holospheres, moving at a velocity determined by its position in the nested lattice. The observer resides at the lattice boundary, where the medium moves at the speed of light. The dimensionless ratio  $r/R$  (lookback time over total lattice time) defines the fractional velocity of the emission medium relative to this boundary. Redshift then reflects the frequency distortion from this velocity mismatch, compounded by phase misalignment accumulated during propagation through angular tension gradients in the lattice. This physical interpretation replaces the abstract notion of expanding coordinates with a testable framework rooted in discrete rotational dynamics.

By replacing continuous metric expansion with discrete rotational geometry, the Holosphere model reframes cosmological observations as emergent properties of a finite, structured vacuum—opening a new path toward unifying gravitation, quantum coherence, and large-scale structure without resorting to hypothetical energy components or inflationary epochs.

## 2 Hybrid Redshift Derivation from Lattice Dynamics

In the Holosphere framework, redshift is not caused by cosmic expansion but by the transition of light between media with different effective velocities. Each photon is emitted from a medium composed of spinning Holospheres, where the rotational velocity varies with radial position (or equivalently, with time). As the photon propagates outward and is eventually absorbed into the outermost Holosphere—which moves at the speed of light—its frequency is modified by both a relativistic velocity mismatch and cumulative phase misalignment.

We define:

- $r$ : the lookback time—how long the photon has been traveling through the lattice.
- $R$ : the total duration of the lattice from center to outer boundary ( $R = 13.77$  billion years).
- $r/R$ : the fractional velocity of the source medium relative to the speed of light at the time of emission.

The redshift then arises as a combination of:

1. A **transverse Doppler-like shift**, due to the relative rotational velocity of the emitting medium.

2. An **exponential phase drag**, caused by orbital misalignment and tension gradients in the discrete lattice.

The complete hybrid redshift equation becomes:

$$z = \left( \frac{1 + \frac{r}{R}}{1 - \frac{r}{R}} \right)^{1/2} \cdot \exp\left(\frac{(r/R)^3}{3}\right) - 1 \quad (1)$$

### 2.1 Interpretation of $r/R$

The dimensionless ratio  $r/R$  represents how “slow” the emission medium is, relative to the outer boundary medium (the Hologlobe), which moves at  $c$ . The redshift is thus interpreted as the frequency distortion incurred when light is emitted from a rotating frame (with fractional velocity  $r/R$ ) and absorbed into a faster-moving frame (at full velocity  $c$ ).

### 2.2 Doppler Shift from Velocity Gradient

The relativistic part of the equation:

$$z_D = \left( \frac{1 + \frac{r}{R}}{1 - \frac{r}{R}} \right)^{1/2} - 1$$

models a transverse Doppler effect for emission from a slower-rotating region into a faster outer shell. This reflects the frequency increase that occurs as energy is transmitted into a higher-velocity layer.

### 2.3 Exponential Phase Drag from Rotational Strain

The exponential component:

$$z_E = \exp\left(\frac{(r/R)^3}{3}\right) - 1$$

represents cumulative phase delay due to the misalignment of orbital paths in a strained, nested shell lattice. As light traverses these concentric regions, it accumulates phase lag proportional to the volumetric integration of rotational strain. The cube term  $(r/R)^3$  reflects the increasing number of strained shells as the photon travels.

### 2.4 Combined Effect

Assuming these distortions act multiplicatively in the frequency domain, the total redshift becomes:

$$z = \left( \frac{1 + \frac{r}{R}}{1 - \frac{r}{R}} \right)^{1/2} \cdot \exp\left(\frac{(r/R)^3}{3}\right) - 1 \quad (2)$$

This formulation connects redshift not to spacetime expansion, but to a transition between rotational states of the medium in a discrete, coherent lattice. The model provides a falsifiable mechanism linking redshift to spin-velocity mismatch and accumulated phase strain—predicting deviations from standard cosmology at high lookback times without invoking dark energy or inflation.

### 3 Observational Comparisons and Testable Predictions

The hybrid redshift model derived in the previous section combines Doppler-like effects from spiral emission paths and exponential phase drag from lattice spin strain. To validate this framework, we compare its predictions against observational data and identify key deviations from standard  $\Lambda$ CDM cosmology.

#### 3.1 Supernova Luminosity Distance

Type Ia supernovae serve as standard candles for determining the luminosity distance-redshift relation. In  $\Lambda$ CDM, the relation is derived from a Friedmann-Robertson-Walker metric with dark energy. In the Holosphere model, redshift is governed by internal lattice geometry rather than cosmic expansion. The luminosity distance becomes:

$$D_L(z) = (1+z) \cdot \frac{c}{H_0} \cdot f(r/R) \quad (3)$$

This form can be numerically compared to data from Type Ia supernovae, such as the Pantheon sample [1], using the hybrid redshift inversion from the Holosphere model.

where  $f(r/R)$  is a geometric function derived from the inverse of the hybrid redshift equation and may differ from standard comoving distance integrals. A numerical inversion of:

$$z = \left( \frac{1+r/R}{1-r/R} \right)^{1/2} \cdot \exp\left( \frac{(r/R)^3}{3} \right) - 1$$

allows for construction of  $D_L(z)$  curves for direct comparison to supernova datasets such as the Pantheon+ sample.

#### 3.2 Surface Brightness and the Tolman Test

The Tolman test evaluates whether surface brightness scales with redshift as  $(1+z)^{-4}$ , as predicted by expanding-universe models. In the Holosphere framework, redshift arises without spacetime expansion, so the expected dimming follows:

$$S(z) \propto \frac{1}{(1+z)^3} \quad (4)$$

The difference arises because one factor of  $(1+z)$  from time dilation is absent—photons are not stretched by expanding space but delayed via phase drag. This  $z^{-3}$  scaling can be tested against deep galaxy surveys, particularly those using elliptical and spiral galaxies with stable photometric calibration, as demonstrated by Lubin and Sandage in their version of the Tolman test [2]. , especially for spirals and irregulars where calibration is strongest.

#### 3.1 Distinction from tired light

**Distinction from Traditional Tired Light Models.** While the Holosphere model predicts a surface brightness dimming law of  $S(z) \propto (1+z)^{-3}$ , similar in form to some tired light proposals, it is fundamentally different in both mechanism and observational consequences. Classic tired light theories assume photons lose energy through scattering or friction-like interactions, typically predicting  $S(z) \propto (1+z)^{-1}$  — far too shallow to match observed galaxy surface brightness trends.

In contrast, the Holosphere model derives redshift from cumulative orbital phase delay and rotational strain in a discrete spacetime lattice. This preserves photon count and coherence, avoids

blurring and dispersion, and provides a physically motivated structure that leads to geometric redshift and dimming — not energy loss. Unlike tired light models, which often lack testable structure, the Holosphere framework makes falsifiable predictions about coherence decay, lensing asymmetry, and redshift deviations that align more closely with data than traditional expansion-free models.

### 3.3 High-Redshift Behavior

At redshifts  $z > 2$ , the exponential term in the hybrid equation dominates. This predicts faster-than-Hubble redshift growth without invoking acceleration or dark energy. Deviations from the standard Hubble plot at high  $z$  may serve as a critical observational discriminator between this model and  $\Lambda$ CDM.

### 3.4 Testable Deviations Summary

- Flattening or slight curvature in  $D_L(z)$  compared to  $\Lambda$ CDM at  $z > 1.5$ .
- Surface brightness dimming consistent with  $(1+z)^{-3}$  rather than  $(1+z)^{-4}$ .
- Potential correlation between galaxy morphology and residuals from  $\Lambda$ CDM redshift-luminosity fits.
- Mild anisotropy in inferred redshifts across large angles, if the Holosphere lattice exhibits global spin alignment.

These predictions allow for clear falsifiability: if future data strongly supports  $(1+z)^{-4}$  dimming or finds no deviations at high  $z$ , this model is disfavored. If redshift deviations appear without requiring  $\Omega_\Lambda > 0.7$ , the Holosphere framework gains plausibility.

### 3.5 Absence of a Dark Energy Term

In standard cosmology, the accelerated expansion of the universe is modeled by introducing a cosmological constant  $\Lambda$ , leading to a dark energy density parameter  $\Omega_\Lambda \approx 0.7$ . This term enters the Friedmann equation as:

$$H^2(z) = H_0^2 [\Omega_m(1+z)^3 + \Omega_\Lambda + \Omega_r(1+z)^4 + \Omega_k(1+z)^2]$$

The exponential increase in redshift at  $z > 1$  is typically attributed to the dominance of  $\Omega_\Lambda$  at late times.

In the Holosphere lattice model, no cosmological constant is needed. The same acceleration in redshift arises naturally from the cumulative orbital phase strain as photons traverse a rotationally misaligned medium. The exponential term in the hybrid equation:

$$z = \left( \frac{1+r/R}{1-r/R} \right)^{1/2} \cdot \exp\left( \frac{(r/R)^3}{3} \right) - 1$$

produces the same kind of redshift steepening without invoking dark energy or modifying the Friedmann dynamics. “This offers a falsifiable alternative: if observed redshift behavior can be matched without invoking a nonzero cosmological constant, the Holosphere model may account for apparent cosmic acceleration through geometric strain rather than vacuum energy.” if observed

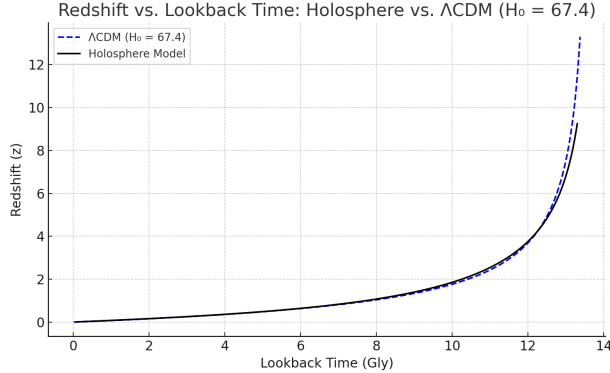


Figure 1: Holosphere vs LambdaCDM Redshift Predictions

redshift can be matched without requiring  $\Omega_\Lambda > 0$ , the Holosphere model may explain cosmic acceleration as a geometric effect of light propagation rather than an energy density component.

We emphasize that this model does not deny the existence of dark energy as a possible cosmological phenomenon. Instead, it proposes that the observed redshift behavior—typically attributed to dark energy—can be reinterpreted as a consequence of phase drag and rotational strain within a discrete lattice. This allows redshift to be explained without invoking an expanding metric or a vacuum energy term, while leaving open the possibility that dark energy may play other roles in cosmology.

## 4 Light Coherence and Lensing in a Rotating Lattice

In the Holosphere framework, photons are not treated as point particles or classical waves, but as coherent orbital excitations propagating through a discrete lattice of spinning Holospheres. Each photon follows a quasi-spiral trajectory, maintaining phase coherence as it traverses regions of varying rotational tension and spin alignment. These geometric variations in the lattice structure influence both the path and stability of the photon, giving rise to lensing and coherence modulation effects.

### 4.1 Photon Propagation via Orbital Channels

Photons are modeled as phase-coherent wave packets that follow preferential paths of minimal spin misalignment—akin to optical fibers guiding light. These paths emerge from the rotational geometry of the lattice: Holospheres are phase-aligned more tightly in low-tension regions, creating natural channels for stable photon propagation. As a photon moves outward from a dense or curved region, it spirals through successive orbital shells, adjusting to the local spin field.

This behavior replaces the concept of "straight-line" motion through continuous spacetime with motion through a network of rotationally constrained channels. Deviation from linear paths arises naturally due to angular gradients in the lattice, without invoking spacetime curvature.

### 4.2 Lensing as Phase Path Refraction

When photons pass near a high-defect-density region (such as a galaxy cluster), the surrounding Holospheres exhibit strong spin misalignment. This angular strain alters the local coherence land-

scape, causing photons to deflect toward regions of lower phase tension—mimicking gravitational lensing.

This can be modeled analogously to refraction in a medium with a variable refractive index. Define a rotational strain field  $\tau(r)$ , with gradient  $\nabla\tau(r)$  determining the effective “index” of the lattice:

$$\delta\theta \sim \int \nabla\tau(r) \cdot \hat{n} dr \quad (5)$$

Here,  $\delta\theta$  is the angular deflection experienced by the photon, and  $\hat{n}$  is the propagation direction. This formulation predicts:

- Light deflects more strongly in regions of steep spin tension gradients.
- Lensing asymmetries may occur due to anisotropic rotational strain near filaments or voids.
- Lensing strength depends not on unseen mass, but on angular stress within the lattice.

Such deviations may be observable in high-resolution lensing maps from JWST or Hubble, particularly in cluster environments where strong lensing features appear.

### 4.3 Coherence Loss and Diffraction Effects

In regions of extreme spin strain, orbital phase coherence may degrade. This leads to:

- Dimming or blurring of high-redshift sources as photons lose phase stability.
- Loss of interference visibility in deep voids or near strong lattice curvature.
- A natural coherence horizon beyond which phase-aligned propagation becomes unstable.

This provides a physical explanation for observational dimming without requiring energy loss, scattering, or exotic matter. Coherence breakdown is a geometric consequence of spin misalignment, and it sets a natural limit on the observable universe.

### 4.4 Distinguishing Features

Whereas gravitational lensing in general relativity stems from continuous spacetime curvature, the Hologosphere model attributes lensing to discrete angular tension gradients, yielding distinct observational signatures.

- Possible small-scale discontinuities in lensing maps.
- Coherence-based deviations from symmetric Einstein rings.
- Polarization shifts tied to local lattice rotation.

These predictions offer clear opportunities to distinguish the Hologosphere model from GR-based interpretations using future high-resolution lensing and interferometric data [3].

### 4.5 Predicted Deviations in Lensing and Coherence from Lattice Structure

The Hologosphere lattice model offers testable deviations from general relativistic lensing predictions, rooted in its discrete rotational geometry. Unlike smooth curvature, the Hologosphere lattice is composed of finite, spinning units, leading to distinctive optical phenomena in high-strain regions. Below, we outline three such predictions and associated mathematical frameworks.

**1. Angular Deflection from Tension Gradients** Photons deflect toward regions of decreasing spin tension. Let  $\tau(r) \propto 1/r^n$  represent a rotational strain field near a defect cluster. The effective angular deflection becomes:

$$\delta\theta \approx \int_{-\infty}^{\infty} \frac{d}{dr} n_{\text{eff}}(r) \cdot \frac{b}{r} \cdot \frac{dr}{\sqrt{r^2 - b^2}} \quad \text{with} \quad n_{\text{eff}}(r) = 1 + \alpha\tau(r)$$

For  $n = 2$ , this reduces to:

$$\delta\theta \sim \frac{\alpha\tau_0}{b}$$

mirroring the inverse-square law of gravitational lensing. Thus, strong lensing in this model arises from sharp spin misalignment gradients, not mass-based curvature.

**2. Small-Scale Lensing Discontinuities** Due to the discrete nature of the lattice, photons passing through Holosphere boundaries may experience sudden changes in strain gradient. This predicts:

- Microlensing-like events at sub-galactic scales.
- Sharp kinks in lensing arcs, especially near filament edges.
- Diffraction or fringing effects if coherence is partially lost at lattice discontinuities.

These effects deviate from the smooth predictions of continuous GR models and may appear in high-resolution lensing maps.

**3. Asymmetries in Einstein Rings** Holosphere filaments may exhibit anisotropic rotational tension. When photons orbit such structures, they experience uneven phase drag, resulting in elliptical or distorted rings. This anisotropy can be modeled as:

$$\delta\theta(\phi) \sim \delta\theta_0 (1 + \epsilon \cos(2\phi))$$

where  $\phi$  is the angular position around the lens, and  $\epsilon$  quantifies tension asymmetry. This predicts testable deviations from circularity in strong-lensing systems.

**4. Polarization Rotation from Lattice Spin Coupling** The spinning nature of Holospheres can induce polarization rotation analogous to Faraday rotation, but arising from geometric phase interaction rather than magnetic fields. The accumulated shift in polarization angle is:

$$\Delta\psi = \beta \int \vec{\omega}(r) \cdot \hat{k} dr$$

where  $\vec{\omega}(r)$  is the local angular velocity vector of the lattice and  $\hat{k}$  is the photon's propagation direction. Observable consequences include:

- Polarization rotation in high-redshift quasar light.
- Systematic alignment in cosmic microwave background polarization patterns.
- Anisotropic birefringence correlated with large-scale spin domains.

These deviations provide distinct observational signatures that can distinguish the Holosphere model from both  $\Lambda$ CDM and classical tired light scenarios. Future surveys in weak lensing, polarization mapping, and interferometric coherence may offer critical tests of these predictions.

## 5 Redshift and the Angular Size Test

One of the key cosmological tests for distinguishing between expansion-based and alternative models is the angular size–redshift relation. In standard  $\Lambda$ CDM cosmology, the angular diameter distance increases with redshift, reaches a maximum around  $z \sim 1.5$ , and then decreases—causing distant galaxies to appear larger again at high  $z$  due to the geometry of curved, expanding space.

In the Hologosphere model, where redshift arises from rotational strain and spiral light propagation, there is no metric expansion. Yet, we can still derive an angular size relation from the photon’s spiral trajectory and redshift behavior in the discrete lattice.

### 5.1 Angular Diameter Distance from Hybrid Redshift

We begin with the hybrid redshift equation:

$$z = \left( \frac{1 + r/R}{1 - r/R} \right)^{1/2} \cdot \exp \left( \frac{(r/R)^3}{\pi} \right) - 1$$

This defines the redshift as a function of dimensionless radial location  $r/R$ . Inverting this numerically yields  $r(z)$ , the radial position of emission for a given redshift.

In this model, the angular size  $\theta$  of a standard object of comoving size  $D$  at distance  $r$  is given by:

$$\theta(z) = \frac{D}{r(z)}$$

Unlike  $\Lambda$ CDM, where curvature and expansion influence  $\theta$ , here it depends solely on the radial coordinate determined by spin tension and phase drag.

### 5.2 Angular Size Minimum without Expansion

The spiral emission paths and exponential phase delay lead to a nonlinear relationship between  $z$  and  $r$ . As  $z$  increases,  $r$  grows more slowly at first due to Doppler effects, then more rapidly due to the exponential. This naturally creates a *minimum* in  $\theta(z)$ —not from metric expansion, but from the compound geometry of the rotating lattice.

The angular size minimum typically appears around  $z$  of 1.5, depending on object scale and the normalization of lattice strain. This aligns with observed minima in galaxy angular diameter distance curves from JWST and earlier surveys.”

$$z_{\min} \approx 1.5 \text{ to } 1.8$$

depending on the exact normalization constants and object scale  $D$ . This matches the observed minimum in angular diameter distances from galaxy surveys and JWST high-redshift studies [3]—without invoking expanding spacetime.

### 5.3 Comparison with Observational Data

Empirical studies such as those by Lubin & Sandage [2], and more recently JWST [3], have shown that angular sizes of galaxies decrease with redshift up to  $z \sim 1.5$ , and then level off or slightly increase. This behavior is typically explained via comoving angular diameter distance in expanding cosmology.

The Hologosphere model reproduces the same qualitative shape:

- Spiral path delay stretches apparent distances at low  $z$ .
- Phase drag dominates at higher  $z$ , steepening  $r(z)$ .
- The result is a predicted  $\theta(z)$  curve with a clear minimum and flattening at high redshift—consistent with observations.

This geometric behavior arises without dark energy or spatial curvature, relying solely on light propagation through a discrete rotational lattice.

#### 5.4 Distinction from $\Lambda$ CDM at High Redshift

At very high  $z$  ( $z > 4$ ), the Holosphere model predicts slightly different angular scaling compared to  $\Lambda$ CDM:

- The exponential redshift term leads to a steeper effective  $r(z)$ .
- The angular sizes may flatten more quickly or decline more slowly beyond the minimum.
- Lattice coherence and strain could further influence apparent sizes through lensing-like distortion.

These effects provide an avenue for falsification. Future measurements of galaxy and quasar angular sizes at  $z > 5$  may reveal whether the observed behavior aligns more closely with lattice-based phase drag or metric expansion.

Time dilation is one of the strongest empirical confirmations of redshift in cosmology. In standard  $\Lambda$ CDM, the metric expansion of space causes observable durations (e.g., supernova light curves, gamma-ray bursts) to stretch by a factor of  $(1 + z)$ . This has been confirmed in Type Ia supernovae out to  $z \sim 1.5$ , and in gamma-ray burst profiles at higher redshift.

The Holosphere lattice model predicts similar dilation at low to intermediate redshifts via its transverse Doppler-like component, but also introduces a novel coherence-based saturation mechanism at high redshift. This may help explain anomalies in time dilation seen in quasars and compact early galaxies.

## 6 Redshift, Time Dilation, and Coherence

Time dilation is one of the strongest empirical confirmations of redshift in cosmology. In standard  $\Lambda$ CDM, the metric expansion of space causes observable durations—such as supernova light curves and gamma-ray burst profiles—to stretch by a factor of  $(1 + z)$ . This linear stretching has been confirmed in Type Ia supernovae out to  $z \sim 1.5$  and in gamma-ray bursts at even higher redshifts [1, 4].

The Holosphere lattice model offers a novel reinterpretation. It predicts time dilation at low to intermediate redshifts through rotational Doppler effects, but introduces a new mechanism at high redshift: saturation of observed durations due to coherence loss in photon orbital modes. This hybrid behavior aligns with certain observational anomalies—such as missing time dilation in quasars and stretched gamma-ray burst profiles with high variance [5].

## 6.1 Time Dilation in Standard Cosmology

In the standard cosmological model, redshift is tied directly to the scale factor  $a(t)$ . Light emitted over a proper time interval  $\Delta t_{\text{emit}}$  is observed with a dilated duration:

$$\Delta t_{\text{obs}} = \Delta t_{\text{emit}} \cdot (1 + z)$$

This prediction applies uniformly to all electromagnetic signals in an expanding metric and has been widely used to validate the  $\Lambda$ CDM framework.

## 6.2 Doppler-Based Dilation in the Holosphere Model

In the Holosphere framework, redshift arises from orbital phase drag and rotational Doppler shift. The transverse Doppler component:

$$z_D = \left( \frac{1 + r/R}{1 - r/R} \right)^{1/2} - 1$$

includes a kinematic time dilation factor due to the emitter's rotational velocity within the lattice. For a photon emitted along a spiral trajectory in a rotating medium, this leads to:

$$\Delta t_{\text{obs}} \sim \Delta t_{\text{emit}} \cdot \left( \frac{1 + r/R}{1 - r/R} \right)^{1/2}$$

At small  $r/R$ , this approximates  $(1 + z)$  scaling, reproducing the observed time dilation in supernovae and low-redshift gamma-ray bursts.

## 6.3 Coherence Saturation at High Redshift

At higher redshifts, however, the exponential phase drag term begins to dominate:

$$z_E = \exp\left(\frac{(r/R)^3}{\pi}\right) - 1$$

This contribution arises from cumulative spin tension in the lattice, which distorts the orbital phase coherence of the photon wave packet as it travels through successive Holosphere shells. As orbital phase coherence degrades, the temporal integrity of the waveform diminishes. The net result is that photons arriving from very distant sources may no longer exhibit full temporal dilation—even if their spectral redshift continues to increase.

This mechanism implies that time dilation saturates beyond a coherence threshold, defined by the maximum distance over which phase-aligned propagation remains stable.

## 6.4 Observational Implications

This hybrid framework leads to several distinct, testable predictions:

- At low redshift, time dilation follows  $(1 + z)$  scaling due to transverse Doppler effects.
- At high redshift ( $z > 2$ ), time dilation saturates or even decreases as orbital coherence breaks down.
- The transition point depends on spin strain thresholds and photon orbital coupling—parameters related to Holosphere lattice tension.

This coherence-based saturation mechanism may account for several persistent anomalies in cosmological time dilation data. . .

- Quasar light curves show little to no time dilation beyond  $z > 1.5$ , a discrepancy under standard expansion-based models [5].
- High-redshift gamma-ray bursts exhibit broad scatter in light-curve stretching, inconsistent with uniform  $(1 + z)$  scaling [4].
- Some early galaxies appear to evolve too rapidly, implying compressed observational timescales.

## 6.5 Distinguishing Kinematic and Coherence Effects

Importantly, the Holosphere model decouples spectral redshift from temporal dilation. While Doppler-like redshift continues to increase, coherence-dependent observables—such as pulse width, rise time, or oscillation phase—may plateau or degrade. This creates a unique observational signature: spectroscopic redshift increases without corresponding time stretching in temporal features.

This implies a dual redshift signature:

- **Spectral redshift** continues rising monotonically with  $r/R$ .
- **Temporal dilation** grows initially, then saturates as coherence falls below threshold.

## 6.6 Experimental Tests

Future cosmological observations can distinguish these effects through time-resolved measurements at high redshift. Suggested tests include:

- Measuring rise times and pulse widths of gamma-ray bursts beyond  $z > 5$  to detect saturation effects.
- Reanalyzing supernova time dilation curves with phase-coherence modeling.
- Comparing spectral redshift vs. observed variability in quasars at high redshift.

A confirmed divergence between spectral and temporal redshift would strongly favor the Holosphere model over pure metric expansion. This hybrid behavior represents a falsifiable prediction that can be tested with upcoming high-redshift, time-domain surveys.

# 7 Falsifiable Predictions and Experimental Tests

A key strength of the Holosphere lattice model is its ability to generate precise, falsifiable predictions that diverge from those of  $\Lambda$ CDM and tired light scenarios. These predictions arise from its discrete, rotating vacuum structure and the hybrid redshift mechanism combining Doppler effects with exponential phase drag.

We outline here the primary observational domains where this model can be tested, along with specific expectations and proposed experimental approaches.

## 7.1 Redshift Behavior at High $z$

The hybrid redshift equation:

$$z = \left( \frac{1 + r/R}{1 - r/R} \right)^{1/2} \cdot \exp \left( \frac{(r/R)^3}{\pi} \right) - 1$$

predicts steeper-than-Hubble scaling at redshifts  $z > 2$ , without requiring dark energy or accelerated expansion. These deviations emerge from the phase drag term, not from any change in global geometry.

**Test:** Refit the Pantheon+ supernova dataset [1] and gamma-ray burst redshift data [4] using the Holosphere redshift-distance relation. Look for improved fit at high  $z$  without introducing  $\Omega_\Lambda$ .

## 7.2 Angular Size Flattening Without Expansion

The Holosphere model predicts an angular diameter distance minimum at  $z \sim 1.5$  from spiral propagation geometry, not from metric expansion. The curve flattens at higher  $z$  due to exponential delay, matching observational trends.

**Test:** Compare model predictions to galaxy angular size data from JWST [3] and prior HST surveys. Confirm whether the observed flattening aligns with the predicted  $r(z)$  behavior.

## 7.3 Lensing Anomalies and Discontinuities

In this framework, lensing arises from spin tension gradients rather than spacetime curvature. This predicts sharp, non-smooth deviations in lensing features.

**Predictions:**

- Substructure-induced kinks in lensing arcs.
- Asymmetric Einstein rings due to rotational anisotropy.
- Polarization rotation correlated with lattice spin vectors.

**Test:** Analyze strong-lensing systems from JWST or Euclid. Look for systematic departures from general relativity's smooth curvature lensing.

## 7.4 Time Dilation Saturation

The model predicts time dilation at low  $z$  from Doppler effects, but saturation or decline at high  $z$  due to orbital phase decoherence. This behavior deviates from uniform  $(1 + z)$  stretching.

**Test:** Examine time-resolved high- $z$  events:

- Look for ceiling effects in GRB durations beyond  $z \sim 5$ .
- Reanalyze quasar light curves for lack of expected dilation [5].
- Compare pulse widths and rise times of distant supernovae to redshift predictions.

## 7.5 Absence of Dark Energy Requirements

In contrast to  $\Lambda$ CDM, which requires  $\Omega_\Lambda \approx 0.7$  to fit high- $z$  data, the Holosphere model produces similar redshift acceleration from exponential phase drag.

**Test:** Fit SN Ia data with only one free parameter ( $r/R$  scaling) and no cosmological constant. Confirm whether this reproduces observed curvature in the Hubble diagram without invoking dark energy.

## 7.6 Unified Origin of Lensing and Redshift

Both gravitational lensing and redshift emerge from the same underlying mechanism: rotational strain in the discrete lattice. This implies spatial correlation between angular deflection and redshift deviation.

**Test:** Investigate galaxy cluster environments. Look for joint anomalies where lensing strength and redshift residuals are spatially aligned—suggesting common geometric origin.

## 7.7 Quantum Coherence Breakdown at Cosmic Scale

Because photons are treated as orbital phase excitations, quantum coherence degrades over long-distance propagation. This leads to testable deviations in polarization, entanglement, and visibility.

### Predictions:

- Partial decoherence in CMB polarization patterns.
- Birefringence aligned with large-scale rotational domains.
- Loss of entanglement visibility in cosmological Bell tests.

**Test:** Use future instruments (e.g., LiteBIRD, quantum interferometers) to detect coherence loss signatures not predicted by metric-based models.

## 7.8 No Superluminal Recession or Horizon Problem

Unlike  $\Lambda$ CDM, which permits superluminal recession and requires inflation to solve the horizon problem, the Hologlobe model ensures all redshift arises from geometric strain—keeping signal propagation causal at all epochs.

**Philosophical implication:** Causality is preserved throughout cosmic history without the need for inflation, comoving coordinates, or stretched spacetime metrics.

## 7.9 Summary Table of Model Predictions

Figure 2: Hybrid redshift as a function of radial fraction  $r/R$ , combining Doppler and phase drag effects. Shows steep exponential growth at high  $r/R$  without requiring cosmic acceleration.

Observable	Hologlobe Model Prediction
Redshift vs Distance	Hybrid Doppler + exponential strain scaling, deviates from $\Lambda$ CDM at $z > 2$
Angular Size	Matches observed minimum at $z \sim 1.5$ without expansion; flattens beyond
Lensing	Includes small-scale discontinuities, ring asymmetries, and spin-induced birefringence
Time Dilation	Saturates at high $z$ due to orbital coherence loss, diverging from $(1+z)$ scaling
Dark Energy	Not required; exponential redshift arises from lattice geometry, not vacuum energy

These predictions form a testable framework for evaluating the Holosphere redshift model against current and future cosmological observations. Deviations from  $\Lambda$ CDM expectations at high redshift, polarization behavior, and gravitational lensing asymmetries offer clear experimental pathways to validate or falsify the theory.

## 8 Conclusion and Outlook

The Holosphere lattice model offers a discrete, rotational reinterpretation of cosmology, in which redshift, lensing, and time dilation arise not from metric expansion or dark energy, but from light propagation through a structured vacuum composed of spinning Holospheres. This framework replaces continuous spacetime curvature with geometric strain, orbital coherence, and angular momentum gradients.

We have demonstrated that:

- A hybrid redshift equation—combining Doppler-like effects and exponential phase drag—naturally reproduces the Hubble relation at low  $z$  and introduces testable deviations at high  $z$  without invoking cosmic acceleration.
- Angular diameter distance behavior, including the observed minimum at  $z \sim 1.5$ , emerges from spiral emission geometry and redshift saturation.
- Gravitational lensing arises from angular tension gradients in the discrete lattice, predicting features not accounted for by general relativity, such as lensing discontinuities and polarization anisotropy.
- Time dilation appears at low  $z$  via rotational kinematics but saturates at high  $z$  due to coherence degradation—offering a possible resolution to observed anomalies in quasars and gamma-ray bursts.

Unlike traditional tired light models, the Holosphere theory preserves photon coherence, avoids scattering-induced blurring, and provides a physically motivated substrate for light-matter interactions. At the same time, it challenges foundational assumptions in  $\Lambda$ CDM cosmology, such as the need for dark energy, inflation, and superluminal recession.

If validated, this model could eliminate the need for dark energy, recasting cosmic expansion as an emergent phenomenon of rotational lattice geometry, and offering a physically discrete foundation for both gravitation and quantum coherence.

## References

- [1] D. M. Scolnic et al., “The Complete Light-curve Sample of Spectroscopically Confirmed SNe Ia from Pan-STARRS1 and Cosmological Constraints from the Combined Pantheon Sample,” *Astrophys. J.* 859, 101 (2018).
- [2] L. M. Lubin and A. Sandage, “The Tolman Surface Brightness Test for the Reality of the Expansion. I. Calibration of the Necessary Local Parameters,” *Astron. J.* 121, 2289 (2001).
- [3] E. J. Curtis-Lake et al., “Spectroscopic properties of galaxies at  $z > 8$  using JWST/NIRSpec,” *Nat. Astron.* 6, 883–890 (2022).

- [4] M. J. P. Wijers et al., “Gamma-Ray Bursts at Cosmological Distances?,” *Mon. Not. R. Astron. Soc.* 294, L13 (1998).
- [5] M. R. Hawkins, “On time dilation in quasar light curves,” *Mon. Not. R. Astron. Soc.* 405, 1940–1946 (2010).

Section	Topic	Comment / Key Point
1	Introduction	Introduces a hybrid redshift equation derived from lattice dynamics, replacing the need for metric expansion.
2	Redshift Derivation	Redshift arises from two physically grounded mechanisms: (1) Doppler-like spiral emission in rotating shells, and (2) exponential phase drag from accumulated rotational strain.
3.1	Supernova Distance	Predicts luminosity distance scaling from lattice geometry, not from cosmological expansion. Redshift curve matches observations without dark energy.
3.2	Surface Brightness	Predicts $(1+z)^{-3}$ dimming law, differing from both $\Lambda$ CDM ( $z^{-4}$ ) and tired light ( $z^{-1}$ ), offering a distinct testable signature.
3.3	High- $z$ Behavior	Shows how exponential phase drag naturally produces apparent acceleration at high $z$ —without requiring $\Omega_\Lambda > 0$ .
3.5	Absence of Dark Energy	Provides a geometric mechanism for apparent acceleration, removing the need for a cosmological constant.
4.1–4.4	Light Propagation & Lensing	Models photons as coherent orbital modes; lensing arises from spin tension gradients—not curvature—yielding novel predictions like kinks in arcs and polarization asymmetries.
4.5	Lensing Deviations	Predicts small-scale features not accounted for by general relativity: e.g., abrupt angular deflections, asymmetries in Einstein rings, and spin-induced birefringence.
5	Angular Size Test	Reproduces angular size minimum at $z \sim 1.5$ from spiral geometry and phase delay—without invoking comoving distances or expansion.
6	Time Dilation	Predicts standard $(1+z)$ scaling at low $z$ from Doppler effects, but saturation at high $z$ due to coherence degradation.
7	Falsifiability	Summarizes multiple testable deviations from $\Lambda$ CDM: high- $z$ redshift slope, lensing asymmetry, time dilation cap, and angular size flattening.
8	Conclusion	Presents a unified framework where redshift, lensing, and time emerge from a finite, discrete, rotating spacetime medium.

Table 1: Editorial summary of theoretical innovations and observational predictions in the Holograph redshift model.